Mon. Not. R. Astron. Soc. **000**, 000–000 (0000) Printed 1 April 2011 (MN LATEX style file v2.2)

The effect of the environment on the HI scaling relations

L. Cortese*[1], B. Catinella[2], S. Boissier[3], A. Boselli[3], S. Heinis[3]
[1] *European Southern Observatory, Karl-Schwarzschild Str. 2, 85748 Garching bei Muenchen, Germany*
[2] *Max-Planck Institut fur Astrophysik, D-85741 Garching bei Muenchen, Germany*
[3] *Laboratoire d'Astrophysique de Marseille, UMR6110 CNRS, 38 rue F. Joliot-Curie, 13388 Marseille, France*

Accepted 2011 March 29. Received 2011 March 28; in original form 2011 March 9

ABSTRACT

We use a volume-, magnitude-limited sample of nearby galaxies to investigate the effect of the environment on the HI scaling relations. We confirm that the HI-to-stellar mass ratio anti correlates with stellar mass, stellar mass surface density and $NUV-r$ colour across the whole range of parameters covered by our sample ($10^9 \lesssim M_* \lesssim 10^{11}$ M$_\odot$, $7.5 \lesssim \mu_* \lesssim 9.5$ M$_\odot$ kpc^{-2}, $2 \lesssim NUV-r \lesssim 6$ mag). These scaling relations are also followed by galaxies in the Virgo cluster, although they are significantly offset towards lower gas content. Interestingly, the difference between field and cluster galaxies gradually decreases moving towards massive, bulge-dominated systems. By comparing our data with the predictions of chemo-spectrophotometric models of galaxy evolution, we show that starvation alone cannot explain the low gas content of Virgo spirals and that only ram-pressure stripping is able to reproduce our findings. Finally, motivated by previous studies, we investigate the use of a plane obtained from the relations between the HI-to-stellar mass ratio, stellar mass surface density and $NUV-r$ colour as a proxy for the HI deficiency parameter. We show that the distance from the 'HI gas fraction plane' can be used as an alternative estimate for the HI deficiency, but only if carefully calibrated on pre-defined samples of 'unperturbed' systems.

Key words: galaxies:evolution–galaxies: fundamental parameters–galaxies: clusters:individual: Virgo–ultraviolet: galaxies– radio lines:galaxies

1 INTRODUCTION

Understanding the role played by the cold gas component in galaxy evolution is one of the main challenges for extragalactic studies. The cold atomic hydrogen (HI) is the reservoir out of which all stars are eventually formed. Therefore a detailed knowledge of its relation to other galaxy properties is of primary importance in order to build a coherent picture of galaxy evolution.

Although the direct detection of HI emission from individual galaxies is still technically limited to the nearby universe (e.g., Verheijen et al. 2007; Catinella et al. 2008), in the last decades several studies have highlighted how the HI content (usually estimated as the HI mass-to-luminosity ratio) varies with morphology, luminosity, size and star formation activity (e.g., Roberts 1963; Haynes & Giovanelli 1984; Roberts & Haynes 1994; Gavazzi et al. 1996; Kannappan 2004; McGaugh & de Blok 1997; Boselli et al. 2001). Particularly powerful appears to be the use of 21 cm data to investigate environmental effects. Several studies have shown that HI-deficient[1] galaxies are mainly/only present in very high-density environments (Giovanelli & Haynes 1985; Cayatte et al. 1990; Solanes et al. 2001; Boselli & Gavazzi 2009), providing strong constraints on the possible environmental mechanisms responsible for the quenching of the star formation in clusters of galaxies (see Boselli & Gavazzi 2006 and references therein).

Unfortunately, a great part of what we know about HI in galaxies has been achieved by studying relatively small samples, with not always well defined selection criteria, often focused on specific morphological classes (e.g., only late-type galaxies) and with small overlap with multiwavelength surveys, necessary to investigate how the cold gas correlates with other baryonic components. Moreover, it is very difficult for simulations to provide accurate estimates for important observables like the HI deficiency parameter (since it is based on a detailed morphological classification), limiting the comparison between observations and theory. In other words, HI astronomy is in a situation similar to the one

* lcortese@eso.org

[1] The HI-deficiency (Def_{HI}) is defined as the difference, in logarithmic units, between the expected HI mass for an isolated galaxy with the same morphological type and optical diameter of the target and the observed value (Haynes & Giovanelli 1984).

of optical and ultraviolet astronomy before the Sloan Digital Sky Survey and the GALEX mission. The main scaling relations (e.g., colour-magnitude, size-luminosity, etc.) were already known, but a detailed quantification of their properties, crucial for a comparison with models, was still missing.

Luckily, the situation is rapidly changing for 21 cm studies. The advent of large HI surveys, such as the *Arecibo Legacy Fast ALFA Survey* (Giovanelli et al. 2005), which eventually will provide HI masses for a few tens of thousands of galaxies over areas of sky with large multiwavelength coverage, is gradually allowing detailed statistical analysis of HI properties in the local universe. Very promising results in this direction have been recently obtained by the *GALEX Arecibo SDSS Survey* (GASS; Catinella et al. 2010), a targeted survey of a volume-limited sample of ∼1000 massive galaxies (M_* >10^{10} $M_\odot$). Catinella et al. (2010) used the first GASS data release to quantify the main scaling relations linking the HI-to-stellar mass ratio to stellar mass, stellar mass surface density and colour. They also suggested the existence of a 'gas fraction plane' linking HI gas fraction[2] to stellar mass surface density and $NUV-r$ colour and proposed to use this plane to isolate interesting outliers that might be in the process of accreting or loosing a significant fraction of their gas content. In this context, the plane might be considered as an alternative way to define HI deficiency when accurate morphological classification is not available. However, this hypothesis has never been tested for a sample for which both HI deficiency and the HI gas fraction plane can be estimated independently.

In this paper, we use a volume-, magnitude-limited sample of ∼300 galaxies to extend the study of the HI scaling relations to a larger dynamical range in stellar mass and stellar mass surface density and to different environments (i.e., from isolated systems to the center of the Virgo cluster). Our main goals are a) to accurately quantify the effect of the cluster environment on the HI scaling relations, b) to investigate the validity of the HI plane as a proxy for HI deficiency and c) to highlight the power of HI scaling relations to constrain models of galaxy formation and evolution.

2 THE SAMPLE

The analysis presented in this paper is based on the Herschel Reference Survey (HRS, Boselli et al. 2010). Briefly, this consists of a volume-limited sample (i.e., 15≤ d ≤25 Mpc) including late-type galaxies (Sa and later) with 2MASS (Skrutskie et al. 2006) K-band magnitude $K_{Stot} \leq 12$ mag and early-type galaxies (S0a and earlier) with $K_{Stot} \leq 8.7$ mag. Additional selection criteria are high galactic latitude (b > +55°) and low Galactic extinction ($A_B < 0.2$ mag, Schlegel et al. 1998), to minimize Galactic cirrus contamination. The total sample consists of 322 galaxies (260 late- and 62 early-type galaxies) [3]. As extensively discussed in Boselli et al. (2010), this sample is not only representative of the local universe but, spanning different density regimes (i.e., from isolated systems to the center of the Virgo cluster), it is also ideal for environmental studies (see also Cortese & Hughes 2009).

Atomic hydrogen masses have been estimated from HI 21 cm line emission data (mainly single-dish), available from the literature (e.g., Springob et al. 2005; Giovanelli et al. 2007; Kent et al. 2008; Gavazzi et al. 2003 and the *NASA/IPAC Extragalactic Database*, NED). In total, 305 out of 322 galaxies in the HRS (∼95%) have been observed at 21 cm, with 265 detections and 40 non detections. HI masses have been computed via

$$\frac{M(HI)}{M_\odot} = 2.356 \times 10^5 \frac{S_{HI}}{\mathrm{Jy\ kms^{-1}}} \Big(\frac{d}{\mathrm{Mpc}}\Big)^2 \quad (1)$$

where S_{HI} is the integrated HI line flux-density and d is the distance. As discussed in Boselli et al. (2010), we fixed the distances for galaxies belonging to the Virgo cluster (i.e., 23 Mpc for the Virgo B cloud and 17 Mpc for all the other clouds; Gavazzi et al. 1999), while for the rest of the sample distances have been estimated from their recessional velocities assuming a Hubble constant H_0 =70 km s^{-1} Mpc^{-1}. In case of non detections, upper limits have been determined assuming a 5σ signal with 300 km s^{-1} velocity width. We estimate the HI deficiency parameter (Def_{HI}) following Haynes & Giovanelli (1984). The expected HI mass for each galaxy is determined via

$$\log(M(HI)_{exp}) = a_{HI} + b_{HI} \times \log\Big(\frac{hD_{25}}{\mathrm{kpc}}\Big) - 2\log(h) \quad (2)$$

where $h = H_0/100$ km s^{-1} Mpc^{-1}, D_{25} is the optical isophotal diameter measured at 25 mag arcsec^2 in B-band and a_{HI} and b_{HI} are two coefficients that vary with morphological type. These coefficients have been calculated for the following types (see also Table 3 in Boselli & Gavazzi 2009): S0a and earlier (Haynes & Giovanelli 1984), Sa-Sab, Sb, Sbc, Sc (Solanes et al. 1996) and Scd to Irr (Boselli & Gavazzi 2009). Morphological classifications for our sample are taken from the Virgo Cluster Catalogue (Binggeli et al. 1985), NED and Boselli et al. (2010). The HI deficiency is then

$$Def_{HI} = \log(M(HI)_{exp}) - \log(M(HI)) \quad (3)$$

We note that the estimate of the expected HI mass for early-type galaxies is extremely uncertain. As we will show later, this uncertainty can significantly affect the quantification of the HI scaling relations. In the following, we will consider as 'HI-deficient' galaxies those objects with $Def_{HI} \geq 0.5$ (i.e., galaxies with 70% less hydrogen than isolated systems with the same diameter and morphological type). The average HI deficiency of galaxies with $Def_{HI} < 0.5$ is Def_{HI}=0.06±0.28, consistent with the typical uncertainty in the estimate of Def_{HI} for isolated field galaxies (Haynes & Giovanelli 1984; Solanes et al. 1996).

Ultraviolet and optical broad-band photometry have been obtained from *Galaxy Evolution Explorer* (GALEX, Martin et al. 2005) and *Sloan Digital Sky Survey* DR7 (SDSS-DR7, Abazajian et al. 2009) databases, respectively. GALEX near-ultraviolet (NUV; λ=2316 Å: $\Delta\lambda$=1069 Å) images have been mainly obtained as part of two ongoing GALEX Guest Investigator programs (GI06-12, P.I. L. Cortese and GI06-01, GUViCS, Boselli et al. 2011). Additional frames have been obtained from the GALEX GR6 public release. All frames have been reduced using the current version of the GALEX pipeline (ops-v7). The GALEX

[2] In this paper we will refer to the $M(HI)/M_*$ ratio as gas fraction.

[3] HRS228/LCRS B123647.4-052325 has been removed from the original sample since the redshift reported in NED was not correct and the galaxy lies well beyond the limits of the HRS, z ∼0.04.

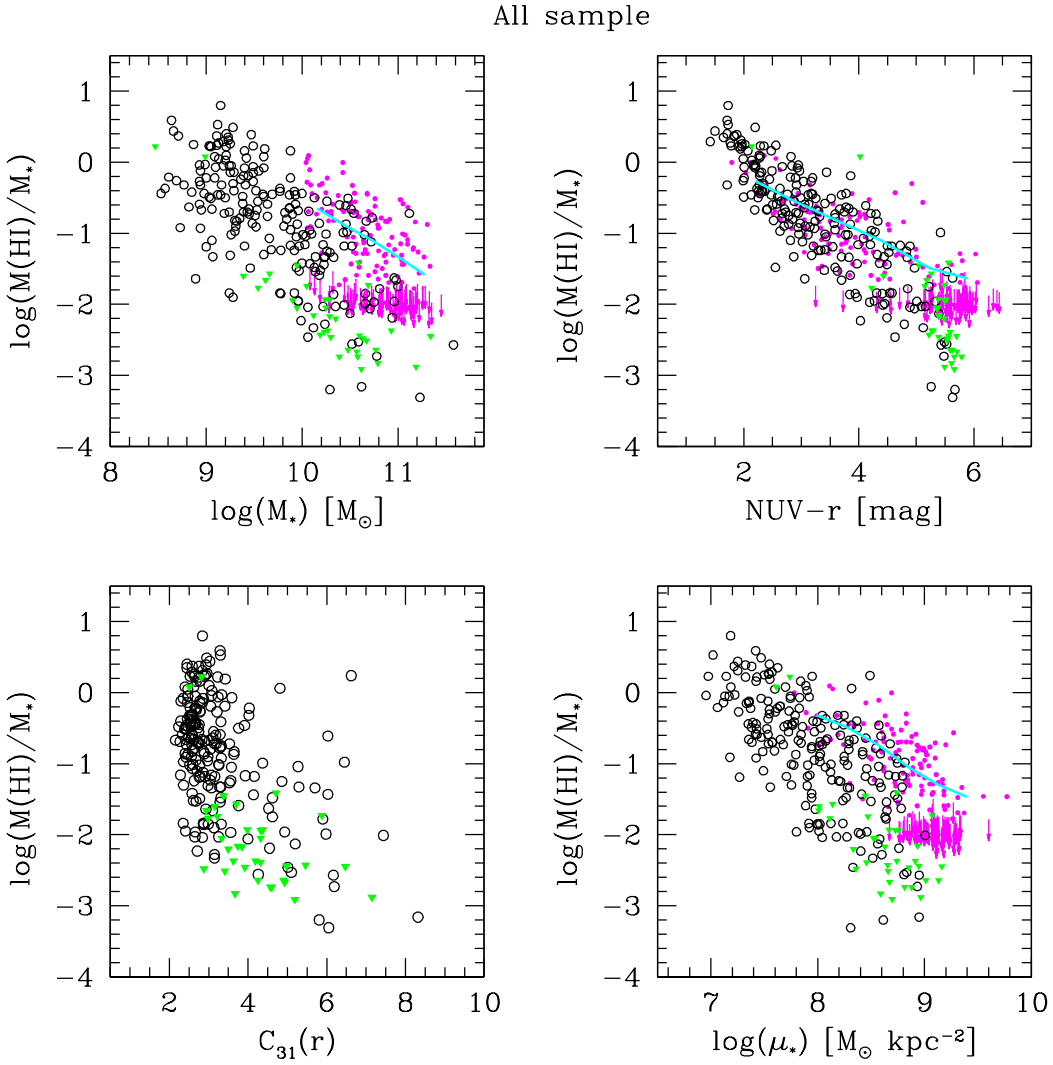

Figure 1. The HI mass fraction of the HRS plotted as a function of stellar mass, $NUV-r$ colour, concentration index and stellar mass surface density. Black circles and green triangles represent detections and non-detections, respectively. GASS DR1 detections and non-detections are indicated with magenta dots and arrows, respectively. The average scaling relations obtained from ALFALFA stacking of the GASS parent sample are indicated in cyan.

NUV and SDSS g,r,i photometry for the HRS was determined as follows. The SDSS images were registered to the GALEX frames and convolved to the NUV resolution (5.3″, Morrissey et al. 2007). Isophotal ellipses were then fit to each image, keeping fixed the center, ellipticity and position angle (generally determined in the i-band). Asymptotic magnitudes have been determined from the growth curve obtained following the technique described by Gil de Paz et al. (2007) and corrected for Galactic extinction assuming a Cardelli et al. (1989) extinction law with $A(V)/E(B-V)$ =3.1: i.e., $A(\lambda)/E(B-V)$=8.2 (Wyder et al. 2007), 3.793, 2.751 and 2.086 for NUV, g, r and i, respectively. Stellar masses M_* are determined from i-band luminosities L_i using the $g-i$ colour-dependent stellar mass-to-light ratio relation from Zibetti et al. (2009), assuming a Chabrier (2003) initial mass function (IMF):

$$\log(M_*/L_i) = -0.963 + 1.032 * (g-i) \qquad (4)$$

The final sample used for the following analysis includes those HRS galaxies for which HI, NUV and SDSS observations are currently available: 241 galaxies (∼75% of the whole HRS, namely 200 late- and 41 early-type galaxies).

3 THE HI SCALING RELATIONS OF THE HRS

In order to quantify how the HI gas fraction varies as a function of integrated galaxy properties, we plot in Fig.1 the HI-to-stellar mass ratio as a function of stellar mass (upper-left panel), observed $NUV-r$ colour (upper-right), concentration index in r-band ($C_{31}(r)$, defined as the ratio between the radii containing 75% and 25% of the total r-band light) and stellar mass surface density (i.e., $M_*/(2\pi R^2_{50,i})$, where $R_{50,i}$ is the radius containing 50% of the total i-band light i.e., the effective radius). For comparison, we also plot the data from the GASS data release 1 (Catinella et al. 2010,

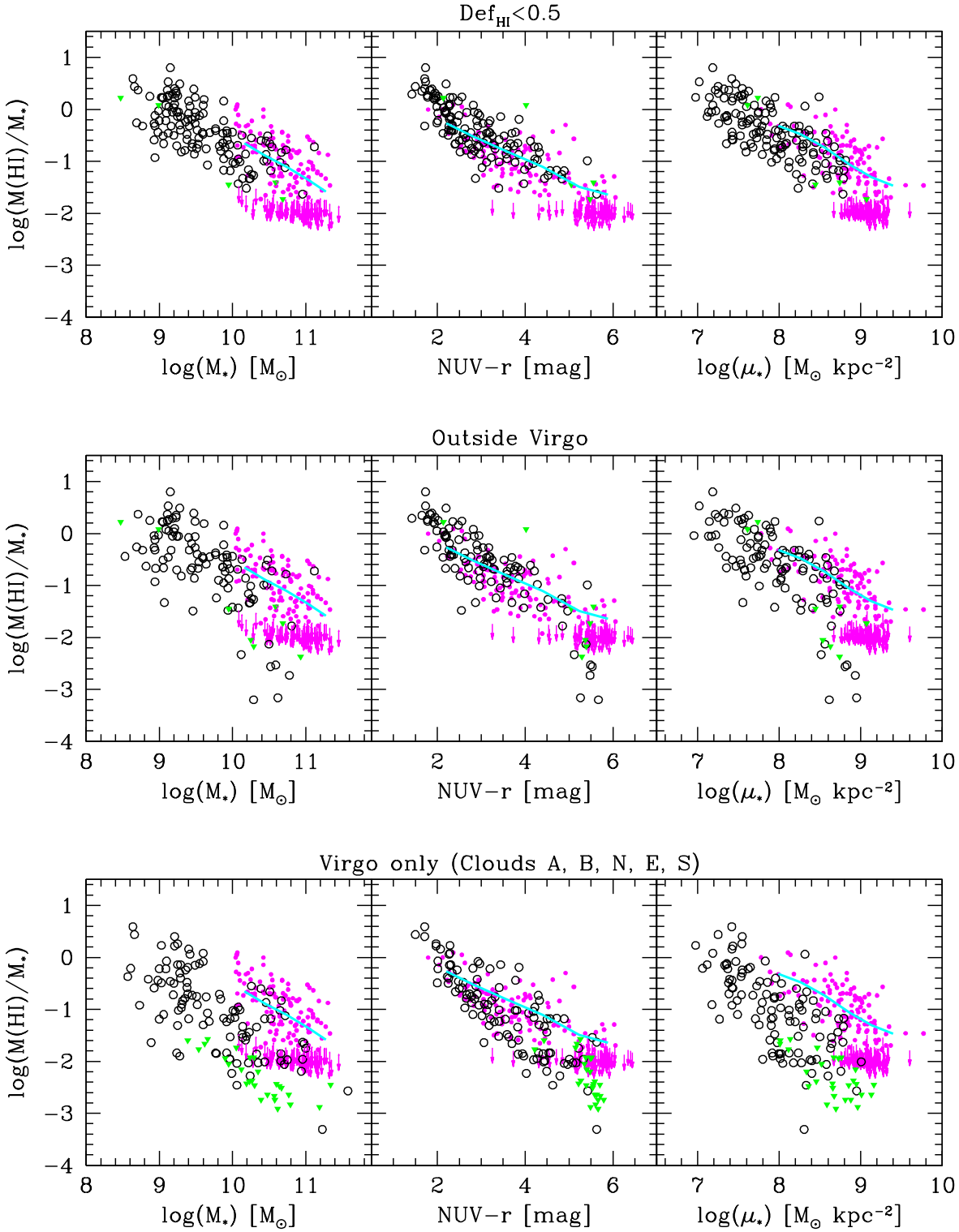

Figure 2. The HI mass fraction as a function of stellar mass, $NUV - r$ colour and stellar mass surface density for HI-normal galaxies (upper panel), galaxies outside the Virgo cluster (middle panel) and galaxies belonging to one of the Virgo cluster clouds (bottom panel). Symbols are as in Fig. 1.

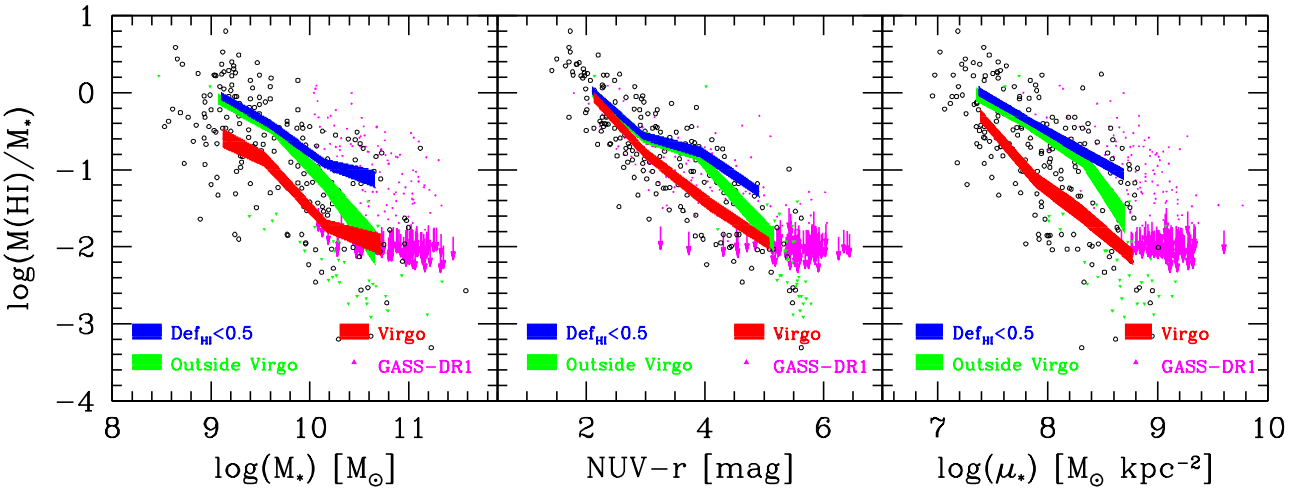

Figure 3. The average HI mass fraction (i.e., $< log(M(HI)/M_*) >$) scaling relations for different samples. HI-normal, galaxies belonging to or outside Virgo are indicated by blue, red and green lines respectively. For comparison, GASS DR1 is shown in magenta.

magenta symbols) and from the stacking of ALFALFA observations for the GASS parent sample (Fabello et al. 2011, cyan line). Over the range of stellar masses covered by the HRS, the HI gas fraction strongly anti-correlates with M_*, $NUV-r$ (a proxy for specific star formation rate, SSFR) and μ_*, while a very weak non-linear trend is observed with the concentration index. The tightest correlation is with the observed $NUV-r$ colour (Pearson correlation coefficient $r=-0.89$, dispersion along the y-axis σ =0.42 dex)[4], while the scatter gradually increases for the stellar surface density ($r=-0.74$, σ =0.61 dex) and mass ($r=-0.72$, σ =0.63 dex).

Our findings extend very nicely the results of the GASS survey (Catinella et al. 2010; Fabello et al. 2011) to lower stellar mass and surface densities, highlighting how the star formation rate, stellar mass and galaxy structure are tightly linked to the HI content of the local galaxy population. However, it is important to notice that the scaling relations for the HRS are slightly offset towards lower gas fractions when compared to the results of the GASS survey. This difference is easily understood when we consider that, by construction, nearly half of the galaxies in the HRS belong to the Virgo cluster and, as a whole, this sample might be biased towards gas-poor objects. To test this and to characterize the HI scaling relations in different environments, we have divided our sample in three different subsets: (a) galaxies with $Def_{HI}<0.5$ (i.e., HI-normal, 135 galaxies), (b) galaxies outside the Virgo cluster (110 galaxies) and (c) galaxies belonging to one of the Virgo cluster clouds (Virgo A, B, N, E and S as defined by Gavazzi et al. 1999, 131 galaxies). We note that, while (b) and (c) are complementary by construction, (a) may include both Virgo and field galaxies. The scaling relations for the three samples are plotted in Fig. 2. As expected, although for all samples the HI gas fraction decreases with stellar mass, colour and stellar mass surface density, galaxies in different environments show significantly different HI content. Virgo galaxies have, on average, a lower HI-to-stellar mass ratio than HI-normal galaxies across the whole range of stellar masses and stellar mass surface densities covered by the HRS. In fact, the dispersion in the two scaling relations drops from ∼0.62 dex for the whole sample to ∼0.37 dex for HI-normal galaxies only.

In order to quantify the difference between cluster and field, in Fig. 3 we show the average trends (i.e., $< log(M(HI)/M_*) >$) for each subsample. The averages are measured by assuming the non detections to their upper-limit and by correcting for the fact that we do not have HI and ultraviolet data for all HRS galaxies. In practice, we weighted each galaxy by the completeness of the sample in its bin of K-band luminosity. The average scaling relations and the number of galaxies contributing to each bin are given in Table 1.

The difference between HI-normal and cluster galaxies varies by ∼0.3 dex as a function of stellar mass (i.e., from ∼0.55 to 0.85 dex), while it increases from ∼0.25 to 1 dex when moving from disk- to bulge-dominated systems (i.e., from $\mu_* \sim 7.4$ to 8.7 $M_\odot$ kpc^{-2})[5]. Less strong is the environmental dependence of the gas fraction vs. $NUV-r$ relation. Blue-sequence galaxies ($NUV-r$ <3.5 mag) have the same HI gas fraction regardless of the environment, consistent with a scenario in which actively star-forming cluster galaxies have just started their infall into the cluster center (Boselli & Gavazzi 2006; Cortese et al. 2008a). On the contrary, red Virgo galaxies are significantly gas poorer than HI-normal systems. It is important to note that this difference might be, at least partially, due to an extinction effect.

[4] These parameters are obtained assuming the non-detections to their upper-limits.

[5] We remind the reader that, by construction, the HRS does not include intermediate-, low-mass early-type galaxies, typically found in high-density environments (Hughes & Cortese 2009; Cortese & Hughes 2009). Thus, for low stellar masses, low stellar mass surface densities and red colours, we might be underestimating the difference between cluster and field galaxies.

While a significant fraction of red cluster galaxies are likely to be really passive systems, field red objects should be more heavily affected by internal dust attenuation. Therefore bins of observed $NUV-r$ colour might not directly correspond to bins of SSFR. We plan to investigate this issue in a future paper, where *Herschel* data will be used to properly correct for internal dust absorption.

Interestingly, we find some differences also when comparing HI-normal galaxies to objects outside the Virgo clusters. Since HI-deficient galaxies are mainly/only found in clusters of galaxies (Haynes & Giovanelli 1984; Cortese et al. 2008b; Boselli & Gavazzi 2009), it is common practice to assume that galaxies in the field, in pairs and loose groups are not HI-deficient (and viceversa). Our analysis shows that a one-to-one correlation between HI-normal galaxies and systems in low-/intermediate-density environments apparently breaks at high stellar masses (M_* >$10^{10.4}$ $M_\odot$), stellar mass surface densities (μ_* > 8.5 $M_\odot$ kpc^{-2}) and red colours ($NUV-r$ >4.5 mag), where we find HI-deficient galaxies also outside the cluster environment. It is important to note that a significant fraction of these gas-poor galaxies (i.e., 5 out of 7 and 6 out of 10 for the $\log(M(HI)/M_*)$ vs. $\log(M_*)$ and $\log(M(HI)/M_*)$ vs. $\log(\mu_*)$ relations, respectively) are early-type systems (S0a or earlier) for which the HI deficiency calibration is notoriously uncertain. Whether the typical red, massive, bulge-dominated galaxy contains a significant cold gas reservoir or not is still matter of debate. These ranges of stellar masses, colour and stellar surface densities have not been adequately sampled by previous HI investigations and it is not completely surprising that we find a difference between HI-normal and field galaxies.

Whatever the origin of the difference between HI-normal and 'field' galaxies, the break observed in the HI scaling relations for galaxies outside the Virgo cluster is very similar to the transition observed in the colour-stellar mass and colour-stellar mass surface density diagrams (e.g., Kauffmann et al. 2003). Bothwell et al. (2009) and Catinella et al. (2010) already reported the presence of a transition in the HI gas fraction vs. stellar mass and stellar mass surface density relations, respectively (see also Kannappan 2004). Our analysis confirms both results at once independently, suggesting that the typical transitions observed in the colour-mass diagram might be related to the transition in HI gas fraction showed in Figs. 2 and 3. Unfortunately, above the transition our statistics becomes too small and we will have to wait for larger HI surveys to characterize more in detail this break in the HI scaling relations.

Finally, it is important to point out that, above the transition in stellar mass/surface density, the difference in HI gas fraction between cluster and field galaxies tends to disappear. This provides an indirect support to a scenario in which environmental effects are today mainly active on the population of low-/intermediate-mass disk galaxies, while the properties of high-mass/bulge-dominated systems are less affected by the local density.

Table 1. The average scaling relations for the three samples discussed in Sec. 3.

HI − normal ($\mathrm{Def_{HI}} < 0.5$)			
x	$< x >$	$< \log(M(HI)/M_*) >^a$	N_{gal}
$\log(M_*)$	9.10	-0.04 ± 0.05	46
	9.59	-0.40 ± 0.06	44
	10.15	-0.92 ± 0.06	31
	10.66	-1.12 ± 0.11	10
$NUV-r$	2.10	$+0.03 \pm 0.05$	52
	2.96	-0.56 ± 0.05	46
	3.93	-0.77 ± 0.07	25
	4.92	-1.29 ± 0.07	9
$\log(\mu_*)$	7.37	$+0.02 \pm 0.06$	36
	7.80	-0.34 ± 0.05	48
	8.30	-0.75 ± 0.07	32
	8.69	-1.06 ± 0.07	16
Outside Virgo			
x	$< x >$	$< \log(M(HI)/M_*) >^a$	N_{gal}
$\log(M_*)$	9.07	-0.08 ± 0.07	36
	9.62	-0.47 ± 0.07	31
	10.14	-1.14 ± 0.12	29
	10.66	-2.00 ± 0.23	11
$NUV-r$	2.10	$+0.01 \pm 0.06$	36
	2.95	-0.57 ± 0.07	34
	3.85	-0.79 ± 0.08	20
	5.17	-1.92 ± 0.15	16
$\log(\mu_*)$	7.35	-0.02 ± 0.09	21
	7.78	-0.37 ± 0.07	40
	8.32	-0.86 ± 0.11	25
	8.70	-1.64 ± 0.18	21
Virgo			
x	$< x >$	$< \log(M(HI)/M_*) >^a$	N_{gal}
$\log(M_*)$	9.12	-0.59 ± 0.12	26
	9.54	-0.86 ± 0.10	33
	10.17	-1.73 ± 0.08	43
	10.72	-1.97 ± 0.14	22
$NUV-r$	2.13	-0.06 ± 0.07	21
	3.00	-0.79 ± 0.07	34
	4.09	-1.45 ± 0.09	32
	5.09	-1.96 ± 0.08	28
$\log(\mu_*)$	7.39	-0.30 ± 0.08	29
	7.89	-1.13 ± 0.10	35
	8.30	-1.56 ± 0.12	34
	8.77	-2.13 ± 0.10	30

a: We note that these are averages of $\log(M(HI)/M_*)$ and not $M(HI)/M_*$ (as in Catinella et al. 2010). We preferred this approach because the distribution of HI gas fraction is closer to a log-normal than to a Gaussian.

4 COMPARISON WITH MODELS

The results presented in § 3 have shown that, at fixed stellar mass and surface densities, cluster galaxies have significantly lower HI-content than galaxies in low density environments. On one side, these results confirm that HI-deficient galaxies are mainly present in high density environments (Haynes & Giovanelli 1984). On the other, they nicely complement previous analysis showing that cluster galaxies have in general a lower star formation rate than their field counterpart (Boselli & Gavazzi 2006; Gavazzi et al. 2002; Gómez et al. 2003), suggesting that the gas loss is behind the quenching of the star formation activity (Gavazzi et al. 2006; Cortese & Hughes 2009). Although this scenario is commonly accepted, there is still

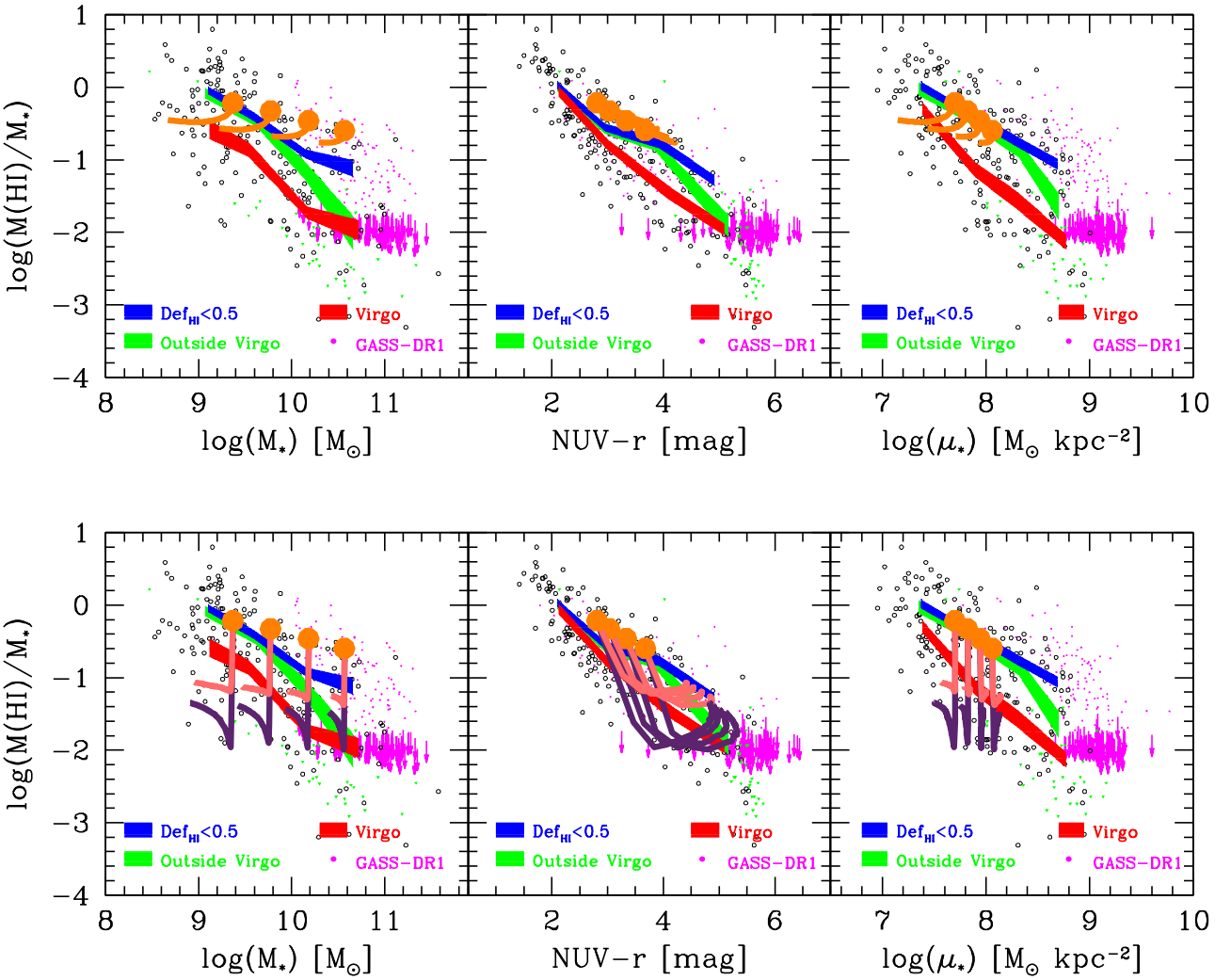

Figure 4. Model predictions for a starvation (upper panels) and ram-pressure stripping (lower panels) event. In case of starvation we considered ages between 0 and 9.5 Gyr, while for ram-pressure we restricted our analysis to events occurred between 0 and 5 Gyr ago. In both sets of panels, the unperturbed model is indicated by the filled circles. In the bottom panel, the two lines indicate models for different ram-pressure efficiencies: ϵ_0 =0.4 (light curve) and 1.2 (dark curve) $M_\odot$ kpc^{-2} yr^{-1}. Data are as in Fig. 3. We note that these are not evolutionary tracks, but illustrate where a galaxy would lie today depending on the age of the interaction.

debate about the environmental mechanism(s) responsible for such differences between low- and high-density environments (e.g., Weinmann et al. 2011). In particular, it is not clear whether the HI is stripped directly from the disk via a strong interaction with the dense intra-cluster medium (i.e., ram-pressure stripping; Gunn & Gott 1972), or if the gas is just removed from the extended gaseous halo surrounding the galaxy, preventing further infall (i.e., starvation; Larson et al. 1980). Boselli et al. (2008) have recently used multi-zone chemical and spectrophotometric models to constrain the evolutionary history of dwarf galaxies in the Virgo cluster and to discriminate between the ram-pressure and starvation scenarios. They showed that the properties of most of the dwarfs dominating the faint end of the Virgo luminosity function are consistent with a scenario in which these galaxies were initially star-forming systems, accreted by the cluster and stripped of their gas by one or more ram pressure stripping events.

Here, we use the same approach adopted by Boselli et al. (2008) to carry out a similar test for intermediate and massive galaxies in the Virgo cluster. The details of the models here adopted can be found in Boselli et al. (2008, Appendix B). Briefly, the evolution of galaxies is traced using the multi-zone chemical and spectrophotometric model of Boissier & Prantzos (2000), updated with an empirically determined star formation law (Boissier et al. 2003) relating the star formation rate to the total gas surface densities. Following Boselli et al. (2008), we modified the original models to simulate the effects induced by the interaction with the cluster environment. In the starvation scenario we simply stopped the infall of pristine gas in the model. We investigate interactions that started between 0 and 9.5 Gyr ago. The ram pressure stripping event is simulated by assuming a gas-

loss rate inversely proportional to the potential of the galaxy, with an efficiency depending on the density of the intracluster medium (taken from Vollmer et al. 2001). We assume two different values for the peak efficiency of ram-pressure stripping (ϵ_0 =0.4 and 1.2 $M_\odot$ kpc^{-2} yr^{-1}) and an age of the interaction between 0 and 5 Gyr ago. Models have been generated assuming a spin parameter λ =0.05 and four different rotational velocities (V_C =100, 130, 170, 220 km s^{-1}), in order to cover the whole range of stellar masses spanned by the HRS. In order to convert the output of the model into the observables here considered, we proceeded as follows. Stellar masses have been converted from a Kroupa et al. (1993), used in the model, to a Chabrier (2003) IMF by adding 0.06 dex (Bell et al. 2003; Gallazzi et al. 2008). Stellar mass surface densities have been determined using the effective radius in i-band, as done for our data. HI masses are obtained from the total gas mass by removing the contribution of helium and heavy elements (i.e., a factor 1.36) and assuming a molecular-to-atomic hydrogen gas ratio of 0.38, independent of stellar mass (Saintonge et al. 2011). $NUV-r$ colours have been 'reddened' by assuming an average internal extinction $A(NUV)$ =1 mag. This value is quite arbitrary and will likely depend on the evolutionary history of each galaxy. However, this assumption does not affect our main conclusions. Finally, we note that the goal of this exercise is to establish which scenario is more consistent with out data, not to determine the best model fitting our observations. There are many free parameters and assumptions in the modeling that could be tweaked in order to better match our observations, but looking for an exact fit does not seem meaningful given the simple description adopted here.

In Fig. 4 (top panels) we compare the predictions of the starvation model with our data. The filled circles indicate the predictions for the unperturbed models. The models seem to fairly reproduce the $NUV-r$ and μ_* vs. gas fraction scaling relations observed for HI-normal and field galaxies. However, a significant difference between data and models is observed in the $M(HI)/M_*$ vs. M_* relation: for very high stellar masses (rotation velocities), the unperturbed model predicts gas fractions ∼0.5 dex higher than the average observed value. This likely reflects the fact that the model is only valid for disk galaxies and does not include any bulge component. It is thus not surprising that at high masses, where the fraction of bulge-dominated galaxies increases, the predictions we obtain are not representative of the whole population (although still well within the range of gas fractions covered by the observations). This is also confirmed by the fact that the model covers just the range of stellar mass surface densities typical of disk galaxies.

By comparing the predictions of the starvation model with our data, it clearly emerges that starvation is only able to mildly affect the HI content, even for very old events. The HI gas fraction decreases by only ≲0.25 dex, i.e. within the intrinsic dispersion of the scaling relation for HI-normal galaxies. This decrease is even lower in the $M(HI)/M_*$ vs. $NUV-r$ plot, where galaxies affected by starvation lie on the main relation observed for unperturbed galaxies. It is thus impossible to reproduce the difference between cluster and field galaxies by just stopping the infall of gas onto the disk.

Much more promising are the results obtained for the ram-pressure stripping model (Fig. 4, bottom panels). For all the three scaling relations here observed, ram-pressure stripping is able to fairly reproduce the difference observed between cluster and field galaxies. A maximum efficiency of 0.4 $M_\odot$ kpc^{-2} yr^{-1} (light curve) is sufficient to reproduce the average decrease in HI content for Virgo galaxies, while a higher efficiency (1.2 $M_\odot$ kpc^{-2} yr^{-1}, dark curve) is necessary to explain some of the most HI-deficient systems in our sample. As expected, the $M(HI)/M_*$ vs. $NUV-r$ is the relation least affected by the environment. Once the gas is removed, the star formation is quickly reduced and the perturbed galaxy will not shift considerably from the main relation. In conclusion, only the direct removal of gas from the star-forming disk is able to reproduce the significant difference between the HI scaling relations of cluster and field galaxies.

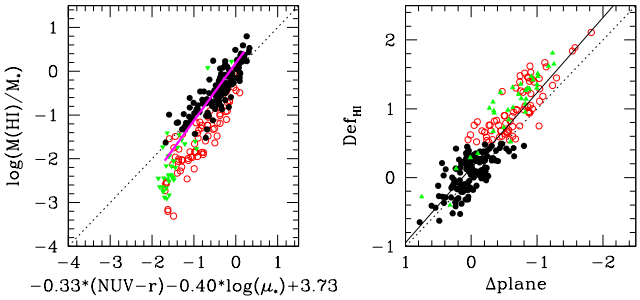

Figure 5. Left panel: The HI gas fraction plane for HI-normal (Def_{HI} <0.5) HRS galaxies.The HI gas fraction plane obtained for GASS galaxies is indicated by the magenta line. Right panel: The correlation between HI deficiency and distance (along the y-axis) from the plane. The solid line indicates the best linear fit to the HI detections. In both panels, HI-normal, HI-deficient galaxies and non-detections are indicated with black filled, red empty circles and green triangles, respectively, and the dotted line shows the 1:1 anti correlation.

5 THE HI GAS FRACTION PLANE AND THE HI DEFICIENCY PARAMETER

In the previous sections we have confirmed the existence of a tight relation between HI gas fraction, stellar mass surface density and $NUV-r$ colour. Recent works have used these three quantities to define a 'gas fraction plane' to be used in order to determine gas fractions for large samples lacking HI observations (Zhang et al. 2009, using optical colours) and to isolate galaxies in the process of accreting or loosing a significant amount of gas (Catinella et al. 2010). As discussed by Zhang et al. (2009), the existence of this plane can be seen as a direct consequence of the Kennicutt-Schmidt relation. In order to test how good the gas fraction plane is as a proxy for HI deficiency, we decided to compare the two approaches for our sample. We thus fitted a plane to the two-dimensional relation between HI mass fraction, stellar mass surface density and $NUV-r$ colour for HI-normal galaxies only (Def_{HI} <0.5), following the methodology outlined in Bernardi et al. (2003), i.e., by minimizing the residuals from the plane. The best fit to the plane is

$$\log\left(\frac{M(HI)}{M_*}\right) = -0.33(NUV-r) - 0.40\log(\mu_*) + 3.73 \quad (5)$$

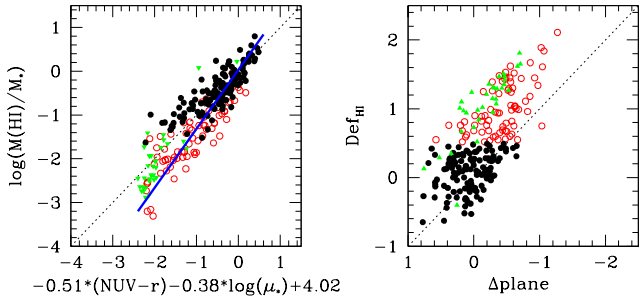

Figure 6. Left panel: The HI gas fraction plane for HRS galaxies outside the Virgo cluster. The HI gas fraction plane obtained for HI-normal HRS galaxies (Fig. 4) is indicated by the solid line. Right panel: The correlation between HI deficiency and distance (along the y-axis) from the plane. Symbols are as in Fig. 5.

and has a dispersion of only ∼0.27 dex, comparable to the typical uncertainty in the HI deficiency parameter. The plane so obtained is illustrated in Fig. 5 (left panel) and is fairly consistent with the one determined for the GASS sample by Catinella et al. (2010, magenta line). Given the different datasets and selection criteria adopted by the two surveys, this agreement is quite remarkable and indicates that both HI-normal HRS and GASS samples provide a fair representation of the HI properties of massive galaxies in the local universe. As expected, HI-deficient galaxies (empty circles) are significantly offset from the plane, having a lower HI-content than what expected for their colour and stellar surface density. The distance from the plane along the y-axis (i.e., $log(M_{HI}/M_*)_{obs} - log(M_{HI}/M_*)_{plane}$) strongly anti correlates with the HI deficiency (Fig. 5, right panel). The best linear fit for the HI detections is

$$Def_{HI} = (-1.09 \pm 0.04) \times \Delta plane + (0.14 \pm 0.02) \quad (6)$$

with ∼0.25 dex dispersion. Again, the scatter is similar to the intrinsic scatter in the definition of the HI deficiency, suggesting that the HI plane is a tool as good as the HI deficiency to isolate extremely HI-rich or HI-poor galaxies, in particular when accurate morphological classification is not available.

Although the results obtained here are very promising, we want to conclude this section with some notes of caution in the definition, and use, of the HI gas fraction plane. The definition of a plane for HI-normal galaxies is justified by the fact that, for this sample, we observe a linear correlation between $\log(M(HI)/M_*)$ and both $NUV - r$ colour and $\log(\mu_*)$. As discussed in the previous section, these linear relations are not valid for typical 'field' galaxies across the whole range of parameter here investigated, but we find a break for massive, bulge-dominated, red galaxies. Therefore, when these objects are included, the concept of a plane is no longer justified. In order to show how important is the sample selection, we plot in Fig. 6 the plane obtained for galaxies outside the Virgo cluster and compare it with what previously obtained for HI-normal galaxies (solid line). The two planes are significantly different, in particular at low HI gas fractions where there is an offset up to a factor ∼4 in the estimate of the HI mass. Incidentally, this shows once more how 'field' galaxies is not the same as 'HI-normal' systems. Moreover, this new plane is almost useless to isolate HI-deficient galaxies. HI-poor systems are no longer strong outliers and the relation between HI deficiency and distance from the plane is too scattered (σ ∼0.4 dex) to be useful. We note that the good agreement between our plane for HI-normal galaxies and the one obtained using GASS detections is due to the fact that both datasets sample the stellar mass surface density regime below the break in HI gas fraction. Notice that, if the GASS detection limit was much deeper than 1.5% gas fraction (which roughly corresponds to the limit separating HI-normal and HI-deficient galaxies at high stellar masses, see Fig. 2), then this survey would include detections above the μ_* break, where the definition of a plane is no longer justified.

In conclusion, the HI gas fraction plane is a promising tool to estimate gas fractions and isolate outliers, but only if calibrated on well defined samples of 'normal' unperturbed galaxies.

6 CONCLUSIONS

In this paper we have shown the relations between HI-to-stellar mass ratio, galaxy structure and colour for the HRS, a volume-, magnitude-limited sample of nearby galaxies. HI gas fractions anti correlate with stellar mass, stellar mass surface density and $NUV - r$ colour, confirming previous results (e.g., Catinella et al. 2010). We show that these trends are observed in both low- and high-density environments, with the only difference that the scaling relations for cluster galaxies are shifted towards lower gas fractions. Thus, the cluster environment seems to have just a secondary (although important) role on galaxy evolution, with the efficiency of gas consumption and star formation mainly driven by the intrinsic 'size' (e.g., total mass) of the system (Gavazzi et al. 1996; Boselli et al. 2001; Kauffmann et al. 2003). Our findings nicely complement the scaling relations between SSFR and galaxy properties revealed by large optical and ultraviolet surveys (Blanton et al. 2005; Schiminovich et al. 2007). Naturally, because the HI is the fuel for star formation, it is likely that the link between SSFR and integrated properties is driven by the scaling relations presented here. This is also supported by the presence of a break in the $M(HI)/M_*$ vs. μ_* and $M(HI)/M_*$ vs. M_* relations, very close to the typical value characterizing the transition between the blue cloud and red sequence.

In order to shed light on the environmental mechanism responsible for the lower HI content of cluster galaxies, we compared our results with the predictions of the chemo-spectrophotometric model by Boissier & Prantzos (2000). We find that simply halting the infall of pristine gas from the halo, mimicking the effect of starvation, is not sufficient to reproduce our observations. Only the stripping of gas directly from the star-forming disk (i.e., ram-pressure) is able to match our data. This naturally explains why HI-deficient galaxies are mainly/only found in very high-density environments, where ram-pressure stripping is efficient. However, it is important to note that our results do not imply that starvation is not playing any role on galaxy evolution. They just show that, if galaxies suffer of starvation, their star formation activity and gas content can be changed, but the shape of the main HI scaling relations will not be significantly altered. We remind the reader that these results are only valid

for disk galaxies. At high masses, where bulge-dominated systems dominate, not only our model cannot be used but, most importantly, the difference between field and cluster starts to disappear, suggesting that the origin of the lower HI content of these objects cannot only be due to the cluster environment.

One of the interesting outcomes of our analysis is that, at high stellar masses, 'field' galaxies are not the same as 'HI-normal' objects. If confirmed, this clear difference might have important implications in our understanding of environmental effects in the local universe. In particular, one of the main issues for environmental studies is to reconcile the evidence that the effects of the environment start at densities typical of poor groups (Blanton & Moustakas 2009 and references therein) with the fact that HI-deficient objects are only observed in clusters of galaxies. Our analysis suggests that, from a statistical point of view, HI-deficient galaxies are clearly segregated in high-density environments only for $M_*\lesssim10^{10}$ $M_\odot$ and $\mu_*\lesssim10^8$ $M_\odot$ kpc^{-2} or, in other words, that intermediate-/low-mass gas-poor quiescent disks are only found in clusters of galaxies. Thus, the results obtained from HI data turn out to be fully consistent with what shown by optical studies: i.e., the intermediate-/low-mass part of the red sequence is only populated in clusters of galaxies (Baldry et al. 2006; Haines et al. 2008; Gavazzi et al. 2010).

Finally, we have confirmed that the HI gas fraction plane defined by Catinella et al. (2010) can be used as an alternative to the HI deficiency parameter. However, we have also illustrated how important is the sample selection in the definition of the HI gas fraction plane and that, as for the HI deficiency, its use is mainly valid for galaxies below the threshold in μ_*.

Our results clearly highlight the importance of HI scaling relations for environmental studies and the necessity to extend this approach to larger samples and to a wider range of environments in order to understand in detail the role played by nurture in galaxy evolution.

ACKNOWLEDGMENTS

We thank the GALEX Time Allocation Committee for the time granted to the HRS and GUViCS projects.

GALEX is a NASA Small Explorer, launched in 2003 April. We gratefully acknowledge NASA's support for construction, operation and science analysis for the GALEX mission, developed in cooperation with the Centre National d'Etudes Spatiales (CNES) of France and the Korean Ministry of Science and Technology.

This publication makes use of data products from Two Micron All Sky Survey, which is a joint project of the University of Massachusetts and the Infrared Processing and Analysis Center/California Institute of Technology, funded by the National Aeronautics and Space Administration and the National Science Foundation.

Funding for the SDSS and SDSS-II has been provided by the Alfred P. Sloan Foundation, the Participating Institutions, the National Science Foundation, the U.S. Department of Energy, the National Aeronautics and Space Administration, the Japanese Monbukagakusho, the Max Planck Society, and the Higher Education Funding Council for England. The SDSS Web Site is http://www.sdss.org/.

The SDSS is managed by the Astrophysical Research Consortium for the Participating Institutions. The Participating Institutions are the American Museum of Natural History, Astrophysical Institute Potsdam, University of Basel, University of Cambridge, Case Western Reserve University, University of Chicago, Drexel University, Fermilab, the Institute for Advanced Study, the Japan Participation Group, Johns Hopkins University, the Joint Institute for Nuclear Astrophysics, the Kavli Institute for Particle Astrophysics and Cosmology, the Korean Scientist Group, the Chinese Academy of Sciences (LAMOST), Los Alamos National Laboratory, the Max-Planck-Institute for Astronomy (MPIA), the Max-Planck-Institute for Astrophysics (MPA), New Mexico State University, Ohio State University, University of Pittsburgh, University of Portsmouth, Princeton University, the United States Naval Observatory, and the University of Washington.

We acknowledge the use of the NASA/IPAC Extragalactic Database (NED) which is operated by the Jet Propulsion Laboratory, California Institute of Technology, under contract with the National Aeronautics and Space Administration and of the GOLDMine data base.

REFERENCES

Abazajian, K. N., Adelman-McCarthy, J. K., Agüeros, M. A., et al. 2009, ApJS, 182, 543
Baldry, I. K., Balogh, M. L., Bower, R. G., et al. 2006, MNRAS, 373, 469
Bell, E. F., McIntosh, D. H., Katz, N., & Weinberg, M. D. 2003, ApJS, 149, 289
Bernardi, M., Sheth, R. K., Annis, J., et al. 2003, AJ, 125, 1866
Binggeli, B., Sandage, A., & Tammann, G. A. 1985, AJ, 90, 1681
Blanton, M. R., Eisenstein, D., Hogg, D. W., Schlegel, D. J., & Brinkmann, J. 2005, ApJ, 629, 143
Blanton, M. R. & Moustakas, J. 2009, ARA&A, 47, 159
Boissier, S. & Prantzos, N. 2000, MNRAS, 312, 398
Boissier, S., Prantzos, N., Boselli, A., & Gavazzi, G. 2003, MNRAS, 346, 1215
Boselli, A., Boissier, S., Cortese, L., & Gavazzi, G. 2008, ApJ, 674, 742
Boselli, A., Boissier, S., Heinis, S., et al. 2011, A&A, 528, 107
Boselli, A., Eales, S., Cortese, L., et al. 2010, PASP, 122, 261
Boselli, A. & Gavazzi, G. 2006, PASP, 118, 517
Boselli, A. & Gavazzi, G. 2009, A&A, 508, 201
Boselli, A., Gavazzi, G., Donas, J., & Scodeggio, M. 2001, AJ, 121, 753
Bothwell, M. S., Kennicutt, R. C., & Lee, J. C. 2009, MNRAS, 400, 154
Cardelli, J. A., Clayton, G. C., & Mathis, J. S. 1989, ApJ, 345, 245
Catinella, B., Haynes, M. P., Giovanelli, R., Gardner, J. P., & Connolly, A. J. 2008, ApJL, 685, L13
Catinella, B., Schiminovich, D., Kauffmann, G., et al. 2010, MNRAS, 403, 683
Cayatte, V., van Gorkom, J. H., Balkowski, C., & Kotanyi, C. 1990, AJ, 100, 604

Chabrier, G. 2003, PASP, 115, 763
Cortese, L., Gavazzi, G., & Boselli, A. 2008a, MNRAS, 390, 1282
Cortese, L. & Hughes, T. M. 2009, MNRAS, 400, 1225
Cortese, L., Minchin, R. F., Auld, R. R., et al. 2008b, MNRAS, 383, 1519
Fabello, S., Catinella, B., Giovanelli, R., et al. 2011, MNRAS, 411, 993
Gallazzi, A., Brinchmann, J., Charlot, S., & White, S. D. M. 2008, MNRAS, 383, 1439
Gavazzi, G., Bonfanti, C., Sanvito, G., Boselli, A., & Scodeggio, M. 2002, ApJ, 576, 135
Gavazzi, G., Boselli, A., Cortese, L., et al. 2006, A&A, 446, 839
Gavazzi, G., Boselli, A., Donati, A., Franzetti, P., & Scodeggio, M. 2003, A&A, 400, 451
Gavazzi, G., Boselli, A., Scodeggio, M., Pierini, D., & Belsole, E. 1999, MNRAS, 304, 595
Gavazzi, G., Fumagalli, M., Cucciati, O., & Boselli, A. 2010, A&A, 517, 73
Gavazzi, G., Pierini, D., & Boselli, A. 1996, A&A, 312, 397
Gil de Paz, A., Boissier, S., Madore, B. F., et al. 2007, ApJS, 173, 185
Giovanelli, R. & Haynes, M. P. 1985, ApJ, 292, 404
Giovanelli, R., Haynes, M. P., Kent, B. R., et al. 2005, AJ, 130, 2598
Giovanelli, R., Haynes, M. P., Kent, B. R., et al. 2007, AJ, 133, 2569
Gómez, P. L., Nichol, R. C., Miller, C. J., et al. 2003, ApJ, 584, 210
Gunn, J. E. & Gott, J. R. I. 1972, ApJ, 176, 1
Haines, C. P., Gargiulo, A., & Merluzzi, P. 2008, MNRAS, 385, 1201
Haynes, M. P. & Giovanelli, R. 1984, AJ, 89, 758
Hughes, T. M. & Cortese, L. 2009, MNRAS, 396, L41
Kannappan, S. J. 2004, ApJL, 611, L89
Kauffmann, G., Heckman, T. M., White, S. D. M., et al. 2003, MNRAS, 341, 54
Kent, B. R., Giovanelli, R., Haynes, M. P., et al. 2008, AJ, 136, 713
Kroupa, P., Tout, C. A., & Gilmore, G. 1993, MNRAS, 262, 545
Larson, R. B., Tinsley, B. M., & Caldwell, C. N. 1980, ApJ, 237, 692
Martin, D. C., Fanson, J., Schiminovich, D., et al. 2005, ApJL, 619, L1
McGaugh, S. S. & de Blok, W. J. G. 1997, ApJ, 481, 689
Morrissey, P., Conrow, T., Barlow, T. A., et al. 2007, ApJS, 173, 682
Roberts, M. S. 1963, ARA&A, 1, 149
Roberts, M. S. & Haynes, M. P. 1994, ARA&A, 32, 115
Saintonge, A., Kauffmann, G., Kramer, C., et al. 2011, MNRAS in press (arXiv:1103.1642)
Schiminovich, D., Wyder, T. K., Martin, D. C., et al. 2007, ApJS, 173, 315
Schlegel, D. J., Finkbeiner, D. P., & Davis, M. 1998, ApJ, 500, 525
Skrutskie, M. F., Cutri, R. M., Stiening, R., et al. 2006, AJ, 131, 1163
Solanes, J. M., Giovanelli, R., & Haynes, M. P. 1996, ApJ, 461, 609
Solanes, J. M., Manrique, A., García-Gómez, C., et al. 2001, ApJ, 548, 97
Springob, C. M., Haynes, M. P., & Giovanelli, R. 2005, ApJ, 621, 215
Verheijen, M., van Gorkom, J. H., Szomoru, A., et al. 2007, ApJL, 668, L9
Vollmer, B., Cayatte, V., Balkowski, C., & Duschl, W. J. 2001, ApJ, 561, 708
Weinmann, S. M., van den Bosch, F. C., & Pasquali, A. 2011, in "Environment and the Formation of Galaxies: 30 years later" Lisbon, 2010, arXiv:1101.3244
Wyder, T. K., Martin, D. C., Schiminovich, D., et al. 2007, ApJS, 173, 293
Zhang, W., Li, C., Kauffmann, G., et al. 2009, MNRAS, 397, 1243
Zibetti, S., Charlot, S., & Rix, H. 2009, MNRAS, 400, 1181